Annals of Solid and Structural Mechanics (2018) 10:17–29
https://doi.org/10.1007/s12356-017-0051-z

ORIGINAL ARTICLE

A mixed explicit–implicit time integration approach for nonlinear analysis of base-isolated structures

Fabrizio Greco[1] · **Raimondo Luciano**[2] · **Giorgio Serino**[3] · **Nicolò Vaiana**[3]

Received: 23 August 2016 / Accepted: 23 November 2017 / Published online: 2 December 2017

Abstract
The paper investigates the accuracy, the stability and the computational efficiency of a mixed explicit–implicit time integration approach proposed for predicting the nonlinear response of base-isolated structures subjected to earthquake excitation. Adopting the central difference method for evaluating the response of the nonlinear base isolation system and the Newmark's constant average acceleration method for estimating the superstructure linear response, the proposed partitioned solution approach is used to analyze a 3D seismically isolated structure subjected to a bidirectional earthquake excitation. Both isolation systems adopting lead rubber and friction pendulum bearings are considered. Numerical results show that the computational time required by the proposed method, in spite of its conditional stability arising from the use of the central difference method in the explicit integration substep, is clearly reduced in comparison to the widely used implicit time integration method adopted in conjunction with the pseudo-force approach (i.e., pseudo-force method). As a matter of fact, the typical low stiffness of the isolation system leads to a critical time step larger than the one used to define the ground acceleration accurately and the proposed method preserves its computational efficiency even in the case of isolators with very high initial stiffness (i.e., friction pendulum bearings) for which the critical time step size could become smaller.

Keywords Base-isolated structures · Mixed time integration · Nonlinear dynamic analysis · Earthquake engineering

1 Introduction

The response of real civil structures subjected to a large dynamic excitation (i.e., blast or seismic loading) often involves significant nonlinear behavior which generally includes the effects of large displacements and/or nonlinear material properties [34].

Direct time integration methods used to solve the nonlinear dynamic equilibrium equations of structures subjected to external excitation (i.e., time-dependent applied forces and/or earthquake excitation) are basically categorized into two groups: explicit and implicit methods. A time integration method is explicit if the solution at time $t + \Delta t$ is obtained by considering the equilibrium conditions at time t and the integration algorithm does not require factorization of the effective stiffness matrix [10]. The method is implicit if the solution at time $t + \Delta t$ is evaluated by considering the equilibrium conditions at time $t + \Delta t$ and a set of simultaneous equations has to be solved at each time step wherein the effective stiffness matrix is a combination of the mass, damping and stiffness matrices [11]. In general, each type of time integration method has its own advantages and disadvantages. Explicit algorithms require a much lower computational effort per time step when compared with implicit methods but are conditionally stable. On the other hand, implicit algorithms can be designed to have unconditional stability, in linear analysis, so that the choice of time step size is limited by accuracy requirements only [2].

In most practical civil engineering problems, the increasing complexity of structural models (i.e., finer finite element mesh, accurate material models) requires the use of a partitioned solution approach in which a discrete structural model is spatially decomposed into interacting components generically called *partitions*. The mathematical foundations of Domain Decomposition Methods (DDMs),

✉ Fabrizio Greco
f.greco@unical.it

[1] Department of Civil Engineering, University of Calabria, Cosenza, Italy

[2] Department of Mechanics, Structures and Environment, University of Cassino, Cassino, Italy

[3] Department of Structures for Engineering and Architecture, University of Naples "Federico II", Naples, Italy

which can be used in the framework of any discretization method for partial differential equations (i.e., finite elements, finite differences) to make their algebraic solution more efficient on parallel computer platforms, can be found in recent numerical analysis texts [29, 30]. The decomposition may be driven by physical or computational considerations [14]. For instance, in the nonlinear soil–structure interaction analysis, being the soil more flexible than the structure, the partitioning of the problem may be a natural choice. In the nonlinear dynamic analysis of a structure subjected to a localized impact, because a small part of the structure is expected to experience strong nonlinear behavior whereas the remaining part would deform into the elastic range, the decomposition of the structural model into two subdomains is driven by computational considerations [5]: in this case, the use of different time steps and time integration methods (i.e., explicit or implicit methods) depending on parts of the analyzed structure instead of adopting a monolithic solution approach (i.e., conventional procedure adopting a single time integration method with a unique time step) can reduce the computational effort significantly.

To overcome the limitations of conventional single-time step integration, partitioned time integration methods have been developed by several authors in the last 30 years to allow different time steps (i.e., multi-time step integration) or time integration algorithms (i.e., mixed time integration) or both to be used in different spatial subdomains of the mesh. Mixed time integration procedures using explicit and implicit time integration methods have been proposed by Hughes and Liu [17], assuming the same time step for all the parts of the mesh. Early works of Belytschko et al. [3] investigated the use of explicit time integration methods with different time steps according to the mesh subdivision and the finite elements size. Wu and Smolinski [35] proposed a new explicit multi-time step integration method for solving structural dynamics problems derived from the modified trapezoidal rule method developed by Pezeshk and Camp [28]. All the previous multi-time step integration methods are essentially based on a nodal partition and prescribe the continuity of displacements, velocities or accelerations at the interface in a strong way, by imposing the equality of subdomain kinematic quantities at the interface. Recently, new methods have been proposed allowing one to prescribe the continuity of those quantities in a weak way by means of Lagrange multipliers [7, 12, 13, 15, 16].

The purpose of this work is to investigate the accuracy, the stability and the computational efficiency of a mixed explicit–implicit time integration method here proposed for predicting the nonlinear response of base-isolated structures subjected to earthquake excitation. Indeed, in the case of seismically isolated structures (i.e., buildings and bridges) the above-mentioned partitioned solution approach can be easily applied being the decomposition of the discrete structural model of such structures driven by physical considerations: the base isolation system is much more flexible than the superstructure to decouple the latter from the earthquake ground motion. Thus, an explicit conditionally stable time integration method can be used to evaluate the base isolation system response and an implicit unconditionally stable time integration method can be adopted to predict the superstructure response with the remarkable benefit in avoiding the iterative procedure within each time step of a nonlinear time history analysis required by conventional implicit time integration methods [32, 33].

The present paper is organized in two parts devoted respectively to the theoretical formulation of the proposed approach and to its numerical applications. In the first part, the dynamic equilibrium equations of the 3D discrete structural model of an actual base-isolated structure are determined (Sect. 2) and the proposed mixed explicit–implicit time integration method is presented (Sect. 3). The explicit method employed is the second order Central Difference Method while the implicit method used is the second order Newmark's Constant Average Acceleration Method. Recently developed time integration algorithms, such as those introduced by Noh and Bathe [25] and Noh et al. [26] for the analysis of wave propagation problems, are not adopted in this work because the main idea is reducing the computational effort required for the solution of nonlinear dynamic equilibrium equations of base-isolated structures, by coupling two of the most widely used time integration methods in the seismic analysis of civil structures. The proposed partitioned solution approach requires firstly the solution of the nonlinear base isolation system response (Explicit Integration Substep), then these results (i.e., base isolation system displacements) are used for the integration of the coupled linear dynamic equilibrium equations of the superstructure (Implicit Integration Substep). In order to evaluate the unknown base isolation system velocity vector in both the Explicit and Implicit Integration Substeps, the three-point backward difference approximation formula is used. The adopted mixed explicit–implicit time integration method is stable as long as stability requirements are fulfilled in the Explicit Integration Substep. Consequently a procedure to evaluate the critical time step is firstly developed for two-dimensional (2D) base-isolated structures and then extended to the three-dimensional (3D) case.

In the second part of the paper (Sect. 4), the proposed theoretical approach is applied to determine the dynamic response of a 3D base-isolated structure subjected to a bidirectional earthquake excitation. Two types of base isolation systems are considered, namely, base isolation system with lead rubber bearings (LRBS) and base isolation system with friction pendulum bearings (FPBS). The latter kind of base isolation system allows one to investigate the use of the mixed time integration procedure also in

the presence of isolators with very high initial stiffness. A mathematical model capable of modeling the biaxial behavior of elastomeric and sliding bearings is adopted and the unconditionally stable semi-implicit Runge–Kutta method [31] is employed to solve the differential equations governing the behavior of each nonlinear isolation element. The accuracy and the computational efficiency of the proposed mixed explicit–implicit method is assessed by comparing the results with those obtained by using the two-step solution algorithm developed specifically for the analysis of base-isolated structures by Nagarajaiah et al. [24]. In this monolithic solution approach, the equations of motion are solved using the implicit unconditionally stable Newmark's constant average acceleration method with the nonlinear forces being represented as pseudo-forces while the differential equations governing the nonlinear behavior of the isolation elements are solved using the Runge–Kutta method. An iterative procedure consisting of corrective pseudo-forces is employed within each time step until equilibrium is achieved. For brevity, in this paper, the above-described implicit time integration method adopted in conjunction with the pseudo-force approach is referred to as the Pseudo-Force Method.

Finally, the main features of the proposed method in terms of accuracy, stability and computational efficiency are summarized in the last section, according to the numerical results obtained in the second part of the paper. As shown, the computational time required by the mixed explicit–implicit time integration method is clearly reduced in comparison to the classical monolithic solution approach (i.e., pseudo-force method). Furthermore, even in the case of base isolation systems having isolators with very high initial stiffness (i.e., sliding bearings) or very high stiffness at large displacements (i.e., high damping rubber bearings) for which the critical time step size could become smaller than the one used to define the ground acceleration accurately, the proposed partitioned solution approach preserves its computational efficiency.

2 Modeling of base-isolated structures

The three-dimensional (3D) discrete structural model of an actual base-isolated structure can be decomposed into two substructures: the superstructure and the base isolation system. The base isolation system consists of seismic isolation bearings called seismic isolators and a full diaphragm above the seismic isolation devices which is generally introduced to distribute the lateral loads uniformly to each bearing [22]. Introducing a flexible base isolation system between the foundation and the superstructure leads to decouple the latter from the earthquake ground motion. In this section, the superstructure and the base isolation system modeling are presented.

2.1 Modeling of the superstructure

The geometry of the 3D discrete structural model of a base-isolated structure is defined in a global, right-handed Cartesian coordinate system, denoted with upper case letters X, Y, and Z, and attached to the center of mass of the base isolation system. The superstructure is considered to remain elastic during the earthquake excitation because it is assumed that the introduction of a flexible base isolation system allows one to reduce the earthquake response in such a way that the superstructure deforms within the elastic range. Each superstructure floor diaphragm (or floor slab) is assumed to be infinitely rigid in its own plane, the columns are assumed to be axially inextensible and the beams are considered to be axially inextensible and flexurally rigid. These kinematics constraints, generally adopted in the literature [6] for beams and columns, are here assumed for simplicity and can be removed straightforwardly without any influence on the generality of the subsequent results. Because of this structural idealization, the total number of a n-story superstructure degrees of freedom (dofs), denoted with nts, is equal to $3n$ and three dofs are referred to the i -th superstructure diaphragm reference point o_i belonging to the horizontal plane of the i-th floor diaphragm and vertically aligned to the global coordinate system origin O. The three dofs of the i-th superstructure diaphragm are the two horizontal translations $u_x^{(i)}$ and $u_y^{(i)}$ in the X and Y directions and the torsional rotation $u_r^{(i)}$ about the vertical axis Z. These three floor diaphragm displacements can be defined relative to the ground or relative to the base isolation system [21]. In this study, the former approach is selected so that the dynamic equilibrium equations of the 3D discrete structural model of an actual base-isolated structure are coupled in terms of elastic and viscous forces and decoupled in terms of inertial forces. The superstructure displacement vector $\boldsymbol{u}_s$, having size nts x 1, is defined by:

$$\boldsymbol{u}_s = \left\{ \boldsymbol{u}_1 \ \cdots \ \boldsymbol{u}_i \ \cdots \ \boldsymbol{u}_n \right\}^T, \tag{1}$$

where:

$$\boldsymbol{u}_1 = \left\{ u_x^{(1)} \ u_y^{(1)} \ u_r^{(1)} \right\}^T \quad \boldsymbol{u}_i = \left\{ u_x^{(i)} \ u_y^{(i)} \ u_r^{(i)} \right\}^T$$
$$\boldsymbol{u}_n = \left\{ u_x^{(n)} \ u_y^{(n)} \ u_r^{(n)} \right\}^T,$$

are the displacement vectors of the first, i-th and n-th superstructure floor diaphragm, respectively.

The superstructure diaphragm mass should include the contributions of the dead load and live load on the floor diaphragm and the contributions of the structural elements (i.e., columns, walls) and of the nonstructural elements (i.e., partition walls, architectural finishes) between floors [6]. The superstructure mass matrix $\boldsymbol{M}_s$ and the i-th superstructure diaphragm mass matrix $\boldsymbol{m}_i$ are:

$$\boldsymbol{M}_s = \begin{bmatrix} \boldsymbol{m}_1 & 0 & 0 \\ 0 & \boldsymbol{m}_2 & 0 \\ & \ddots & \\ 0 & 0 & \boldsymbol{m}_n \end{bmatrix}, \quad \boldsymbol{m}_i = \begin{bmatrix} m^{(i)} & 0 & -S^{(i)}_x \\ 0 & m^{(i)} & S^{(i)}_y \\ -S^{(i)}_x & S^{(i)}_y & I^{(i)}_o \end{bmatrix}, \tag{2}$$

where $m^{(i)}$ is the i-th diaphragm mass, $S^{(i)}_x$ and $S^{(i)}_y$ are the first moments of the i-th diaphragm mass about the global horizontal axes X and Y, respectively, and $I^{(i)}_o$ is the moment of inertia of the i-th diaphragm about the global vertical axis Z. If the mass center of the i-th floor diaphragm and the origin of the global coordinate system O are aligned vertically the superstructure diaphragm mass matrix is diagonal.

The superstructure stiffness matrix $\boldsymbol{K}_s$ and the i-th superstructure story stiffness matrix $\boldsymbol{k}_i$ are:

$$\boldsymbol{K}_s = \begin{bmatrix} \boldsymbol{k}_1 + \boldsymbol{k}_2 & -\boldsymbol{k}_2 & & 0 \\ -\boldsymbol{k}_2 & \boldsymbol{k}_2 + \boldsymbol{k}_3 & \ddots & \\ & \ddots & \ddots & -\boldsymbol{k}_n \\ 0 & & -\boldsymbol{k}_n & \boldsymbol{k}_n \end{bmatrix}, \quad \boldsymbol{k}_i = \begin{bmatrix} k^{(i)}{}_{xx} & k^{(i)}{}_{xy} & -k^{(i)}{}_{xr} \\ k^{(i)}{}_{yx} & k^{(i)}{}_{yy} & k^{(i)}{}_{yr} \\ -k^{(i)}{}_{xr} & k^{(i)}{}_{yr} & k^{(i)}{}_{rr} \end{bmatrix}, \tag{3}$$

where $k^{(i)}{}_{xx}$, $k^{(i)}{}_{xy}$ and $k^{(i)}{}_{xr}$ are the resulting elastic forces in X direction of the i-th superstructure story due to unit translation in X and Y directions and unit torsional rotation of the i-th superstructure diaphragm about the vertical axis Z, respectively; $k^{(i)}{}_{yy}$, $k^{(i)}{}_{yx}$ and $k^{(i)}{}_{yr}$ are the resultants of the elastic forces in Y direction of the i-th superstructure story due to unit translation in Y and X directions and unit torsional rotation of the i-th superstructure diaphragm about the vertical axis Z, respectively; and $k^{(i)}{}_{rr}$ is the resultant of the elastic torsional moment of the i-th superstructure story due to unit torsional rotation of the i-th superstructure diaphragm about the vertical axis Z. The torsional stiffness of each individual resisting vertical element (i.e., column or wall) is considered negligible [18].

Classical damping is an appropriate idealization if similar damping mechanisms are distributed throughout the superstructure. In order to construct a classical damping matrix from modal damping ratios the Rayleigh damping can be assumed allowing one to express the damping matrix in terms of the superstructure mass and stiffness matrices:

$$\boldsymbol{C}_s = \alpha_0 \boldsymbol{M}_s + \alpha_1 \boldsymbol{K}_s \,. \tag{4}$$

The Rayleigh damping coefficients α_0 and α_1 can be selected to match the desired damping ratio for two modes, oftentimes the two lowest, but not always [4]. Denoting these modes as the f-th and the s-th, it is possible to write:

$$\begin{aligned} \alpha_0 + \alpha_1 \, \omega_f^2 &= 2 \, \zeta_f \, \omega_f \\ \alpha_0 + \alpha_1 \, \omega_s^2 &= 2 \, \zeta_s \, \omega_s \end{aligned} .$$

With given damping ratios ζ_f and ζ_s these two equations can be solved for α_0 and α_1.

2.2 Modeling of the base isolation system

The base isolation system diaphragm is assumed to be infinitely rigid in its own plane, the beams are considered to be axially inextensible and flexurally rigid and the seismic isolators are assumed to be infinitely rigid in the vertical direction. As a result of these kinematic constraints, the total number of the base isolation system dofs, denoted with *ntb*, is equal to 3. These three dofs, which are attached to the mass center of the base diaphragm and are defined relative to the ground, are the two horizontal translations $u^{(b)}_x$ and $u^{(b)}_y$ in the X and Y directions and the torsional rotation $u^{(b)}_r$ about the vertical axis Z. The isolation system displacement vector $\boldsymbol{u}_b$, having size *ntb x* 1, is:

$$\boldsymbol{u}_b = \left\{ u^{(b)}_x \;\; u^{(b)}_y \;\; u^{(b)}_r \right\}^T. \tag{5}$$

The base isolation system mass matrix $\boldsymbol{m}_b$ is defined by:

$$\boldsymbol{m}_b = \begin{bmatrix} m^{(b)} & 0 & 0 \\ 0 & m^{(b)} & 0 \\ 0 & 0 & I^{(b)}_o \end{bmatrix}, \tag{6}$$

where $m^{(b)}$ is the diaphragm mass and $I^{(b)}_o$ is the moment of inertia of the diaphragm about the global vertical axis Z. The two first moments $S^{(b)}_x$ and $S^{(b)}_y$ of the base diaphragm mass about the global horizontal axes X and Y are equal to zero because the diaphragm mass center and the origin of the global coordinate system O are coincident.

The base isolation system can include linear isolation elements and nonlinear isolation elements. Considering the linear elements (i.e., seismic isolators whose behavior can be modeled by a linear spring and a linear viscous damper in parallel), the base isolation system stiffness matrix $\boldsymbol{k}_b$ is:

$$\boldsymbol{k}_b = \begin{bmatrix} k^{(b)}{}_{xx} & k^{(b)}{}_{xy} & -k^{(b)}{}_{xr} \\ k^{(b)}{}_{yx} & k^{(b)}{}_{yy} & k^{(b)}{}_{yr} \\ -k^{(b)}{}_{xr} & k^{(b)}{}_{yr} & k^{(b)}{}_{rr} \end{bmatrix}, \tag{7}$$

where $k^{(b)}{}_{xx}$, $k^{(b)}{}_{xy}$ and $k^{(b)}{}_{xr}$ are the resultants of the elastic forces in X direction of the linear elements due to unit translation in X and Y directions and unit torsional rotation of the base diaphragm about the vertical axis Z, respectively; $k^{(b)}{}_{yy}$, $k^{(b)}{}_{yx}$ and $k^{(b)}{}_{yr}$ are the resultants of the elastic forces in Y direction of the linear elements due to unit translation in Y and X directions and unit torsional rotation of the base diaphragm about the vertical axis Z, respectively; and $k^{(b)}{}_{rr}$ is the resultant elastic torsional moment of the linear elements due to unit torsional rotation of the base diaphragm about the vertical axis Z. The torsional stiffness of the seismic isolators is negligible and is not included [19].

The base isolation system viscous damping matrix $\boldsymbol{c}_b$ is:

$$\boldsymbol{c}_b = \begin{bmatrix} c^{(b)}{}_{xx} & 0 & 0 \\ 0 & c^{(b)}{}_{yy} & 0 \\ 0 & 0 & c^{(b)}{}_{rr} \end{bmatrix}, \tag{8}$$

where $c^{(b)}{}_{xx}$ and $c^{(b)}{}_{yy}$ are the resultants of the viscous damping forces in X and Y directions, respectively, of the linear elements due to unit velocity of the base diaphragm in X and Y directions and $c^{(b)}{}_{rr}$ is the resultant of the viscous damping torsional moment of the linear elements due to unit rotational velocity of the base diaphragm about the vertical axis Z. The off-diagonal terms of the base isolation system viscous damping matrix are neglected [1].

As far as the nonlinear elements is concerned, the resultant nonlinear forces vector of the base isolation system $\boldsymbol{f}_n$ is:

$$\boldsymbol{f}_n = \begin{Bmatrix} f_{nx} \\ f_{ny} \\ f_{nr} \end{Bmatrix}, \tag{9}$$

where f_{nx}, f_{ny} and f_{nr} are the resultant nonlinear forces in X and Y directions and the resultant nonlinear torsional moment about the vertical axis Z of the nonlinear elements. The nonlinear behavior of each seismic isolator can be modeled using an explicit nonlinear force–displacement relation [24].

2.3 Dynamic equilibrium equations

The equations of motion of the 3D discrete structural model of an actual base-isolated structure are:

$$\begin{aligned} &\begin{bmatrix} \boldsymbol{m}_b & 0^T \\ 0 & \boldsymbol{M}_s \end{bmatrix} \begin{Bmatrix} \ddot{\boldsymbol{u}}_b \\ \ddot{\boldsymbol{u}}_s \end{Bmatrix} + \begin{bmatrix} \boldsymbol{c}_b + \boldsymbol{c}_1 & \boldsymbol{c}^T \\ \boldsymbol{c} & \boldsymbol{C}_s \end{bmatrix} \begin{Bmatrix} \dot{\boldsymbol{u}}_b \\ \dot{\boldsymbol{u}}_s \end{Bmatrix} \\ &+ \begin{bmatrix} \boldsymbol{k}_b + \boldsymbol{k}_1 & \boldsymbol{k}^T \\ \boldsymbol{k} & \boldsymbol{K}_s \end{bmatrix} \begin{Bmatrix} \boldsymbol{u}_b \\ \boldsymbol{u}_s \end{Bmatrix} \\ &+ \begin{Bmatrix} \boldsymbol{f}_n \\ 0 \end{Bmatrix} = -\begin{bmatrix} \boldsymbol{m}_b & 0^T \\ 0 & \boldsymbol{M}_s \end{bmatrix} \begin{bmatrix} \boldsymbol{R}_b \\ \boldsymbol{R}_s \end{bmatrix} \ddot{\boldsymbol{u}}_g, \end{aligned} \tag{10}$$

with

$$\boldsymbol{c} = \begin{bmatrix} -\boldsymbol{c}_1 & 0 \end{bmatrix}^T, \qquad \boldsymbol{k} = \begin{bmatrix} -\boldsymbol{k}_1 & 0 \end{bmatrix}^T,$$
$$\ddot{\boldsymbol{u}}_g = \begin{Bmatrix} \ddot{u}_{gx} & \ddot{u}_{gy} & 0 \end{Bmatrix}^T,$$

where $\boldsymbol{c}_1$ and $\boldsymbol{k}_1$ are the first superstructure story viscous damping and stiffness matrices, $\boldsymbol{R}_b$ and $\boldsymbol{R}_s$ are the base isolation system and superstructure influence matrices, and $\ddot{\boldsymbol{u}}_g$ is the ground (or support) acceleration vector in which $\ddot{u}_{gx}$ and $\ddot{u}_{gy}$ are the X and Y ground acceleration components while the rotational component is neglected.

The system of $3n + 3$ coupled Ordinary Differential Equations (ODEs) of the second order in time is nonlinear because of the presence of the resultant nonlinear forces vector of the base isolation system $\boldsymbol{f}_n$. In the monolithic solution approach proposed by [24], developed specifically for base-isolated structures and referred to as the Pseudo-Force Method in this paper, the equations of motion are discretized using the implicit unconditionally stable Newmark's Constant Average Acceleration Method. As the nonlinear forces vector $\boldsymbol{f}_n$ could be function of both displacement and velocity vectors at time $t + \Delta t$, according to the model adopted for each seismic isolator (i.e., Bouc–Wen Model), it is transferred to the right hand side of Eq. (10) and treated as pseudo-forces vector. Thus, an iterative procedure consisting of corrective pseudo-forces has to be adopted within each time step until equilibrium is achieved.

3 Mixed explicit–implicit time integration method

In this section, a mixed explicit–implicit time integration method is proposed for analyzing base-isolated structures subjected to earthquake excitation. The solution algorithm is characterized by two substeps called *Explicit Integration Substep* and *Implicit Integration Substep*, respectively. In each time step of a nonlinear time history analysis, the nonlinear response of the base isolation system is computed first using the explicit time integration method, then the implicit method is adopted to evaluate the superstructure linear response. The solution algorithm is summarized in the Appendix for use in a computer program.

3.1 Explicit integration substep

The explicit time integration method adopted to predict the response of the base isolation system is the second order central difference method which is one of the most used among explicit methods in structural dynamics programs and is said to have the highest accuracy and maximum stability limit for any explicit method of order two [20].

In the explicit integration substep, the equations of motion at time t are used to evaluate the base isolation system displacement vector $\boldsymbol{u}_b$ for time $t + \Delta t$. Hence, writing the first set of *ntb* dynamic equilibrium equations of the 3D discrete structural model at time t gives:

$$\begin{aligned} &\boldsymbol{m}_b \ddot{\boldsymbol{u}}_b(t) + \left(\boldsymbol{c}_b + \boldsymbol{c}_1\right) \dot{\boldsymbol{u}}_b(t) + \boldsymbol{c}^T \dot{\boldsymbol{u}}_s(t) + \left(\boldsymbol{k}_b + \boldsymbol{k}_1\right) \boldsymbol{u}_b(t) \\ &\quad + \boldsymbol{k}^T \boldsymbol{u}_s(t) + \boldsymbol{f}_n\left(\boldsymbol{u}_b(t), \dot{\boldsymbol{u}}_b(t)\right) = -\boldsymbol{m}_b \boldsymbol{R}_b \ddot{\boldsymbol{u}}_g(t). \end{aligned} \tag{11}$$

This method is based on a finite difference approximation of the time derivatives of displacement (i.e., velocity and acceleration). Taking constant time steps, the central difference expressions for velocity and acceleration vectors at time t are:

$$\dot{\boldsymbol{u}}_b(t) = \frac{1}{2\Delta t}\left[\boldsymbol{u}_b(t+\Delta t) - \boldsymbol{u}_b(t-\Delta t)\right], \tag{12}$$

$$\ddot{\boldsymbol{u}}_b(t) = \frac{1}{(\Delta t)^2}\left[\boldsymbol{u}_b(t+\Delta t) - 2\boldsymbol{u}_b(t) + \boldsymbol{u}_b(t-\Delta t)\right]. \tag{13}$$

The error in the expressions (12) and (13) is of order $(\Delta t)^2$, so the error in $\boldsymbol{u}_b$ is quartered when Δt is halved.

Substituting the relations for $\dot{\boldsymbol{u}}_b(t)$ and $\ddot{\boldsymbol{u}}_b(t)$, from (12) and (13), respectively, into Eq. (11), and rearranging terms, gives:

$$\begin{aligned}\left[\frac{1}{(\Delta t)^2}\boldsymbol{m}_b + \frac{1}{2\Delta t}\left(\boldsymbol{c}_b + \boldsymbol{c}_1\right)\right]\boldsymbol{u}_b(t+\Delta t)\\ = -\boldsymbol{m}_b\boldsymbol{R}_b\ddot{\boldsymbol{u}}_g(t) - \boldsymbol{c}^T\dot{\boldsymbol{u}}_s(t) - \boldsymbol{k}^T\boldsymbol{u}_s(t) - \boldsymbol{f}_n\left(\boldsymbol{u}_b(t), \dot{\boldsymbol{u}}_b(t)\right)\\ + \left[\frac{2}{(\Delta t)^2}\boldsymbol{m}_b - \boldsymbol{k}_b - \boldsymbol{k}_1\right]\boldsymbol{u}_b(t)\\ + \left[-\frac{1}{(\Delta t)^2}\boldsymbol{m}_b + \frac{1}{2\Delta t}\left(\boldsymbol{c}_b + \boldsymbol{c}_1\right)\right]\boldsymbol{u}_b(t-\Delta t),\end{aligned} \tag{14}$$

from which $\boldsymbol{u}_b(t+\Delta t)$ can be evaluated.

In Eq. (14), $\boldsymbol{u}_b(t-\Delta t)$, $\boldsymbol{u}_b(t)$, $\boldsymbol{u}_s(t)$ and $\dot{\boldsymbol{u}}_s(t)$ are assumed known from implementation of the procedure for the preceding time steps. In order to calculate the solution at time Δt, a special starting procedure must be used. Since $\boldsymbol{u}_b(0)$, $\dot{\boldsymbol{u}}_b(0)$ and $\ddot{\boldsymbol{u}}_b(0)$ are known at time $t = 0$, $\boldsymbol{u}_b(-\Delta t)$ can be obtained using the following relation [2]:

$$\boldsymbol{u}_b(-\Delta t) = \boldsymbol{u}_b(0) - \Delta t\,\dot{\boldsymbol{u}}_b(0) + \frac{(\Delta t)^2}{2}\ddot{\boldsymbol{u}}_b(0). \tag{15}$$

The resultant nonlinear forces vector of the base isolation system $\boldsymbol{f}_n$ depends on the response at time t and could be function of both displacement and velocity, according to the explicit nonlinear force–displacement relation used to model each seismic isolator. The base isolation system velocity vector at time t can be evaluated in terms of displacement vectors using the three-point backward difference approximation [9]:

$$\dot{\boldsymbol{u}}_b(t) = \frac{1}{2\,\Delta t}\left[-4\,\boldsymbol{u}_b(t-\Delta t) + 3\boldsymbol{u}_b(t) + \boldsymbol{u}_b(t-2\Delta t)\right]. \tag{16}$$

The error in the expression (16) is of order $(\Delta t)^2$. It is worth noting that the base isolation system velocity vector at time t can not be determined by using Eq. (12) because $\boldsymbol{u}_b(t+\Delta t)$ is unknown.

3.2 Implicit integration substep

The implicit time integration method adopted to compute the linear response of the superstructure is the second order Newmark's constant average acceleration method which is one of the most effective and popular implicit methods, especially for the linear and nonlinear time history analysis of civil structures.

In the implicit integration substep, the equations of motion at time $t + \Delta t$ are used to evaluate the superstructure displacement vector $\boldsymbol{u}_s$ for time $t + \Delta t$. Hence, writing the second set of *nts* dynamic equilibrium equations of the 3D discrete structural model at time $t + \Delta t$ gives:

$$\begin{aligned}\boldsymbol{M}_s\ddot{\boldsymbol{u}}_s(t+\Delta t) + \boldsymbol{C}_s\dot{\boldsymbol{u}}_s(t+\Delta t) + \boldsymbol{K}_s\boldsymbol{u}_s(t+\Delta t)\\ + \boldsymbol{c}\dot{\boldsymbol{u}}_b(t+\Delta t) + \boldsymbol{k}\boldsymbol{u}_b(t+\Delta t) = -\boldsymbol{M}_s\boldsymbol{R}_s\ddot{\boldsymbol{u}}_g(t+\Delta t).\end{aligned} \tag{17}$$

This method is based on the assumption that the variation of acceleration over a time step is constant, equal to the average acceleration. Taking constant time steps, the expressions for the superstructure velocity and acceleration vectors at time $t + \Delta t$ are:

$$\dot{\boldsymbol{u}}_s(t+\Delta t) = \frac{2}{\Delta t}\left[\boldsymbol{u}_s(t+\Delta t) - \boldsymbol{u}_s(t)\right] - \dot{\boldsymbol{u}}_s(t), \tag{18}$$

$$\ddot{\boldsymbol{u}}_s(t+\Delta t) = \frac{4}{(\Delta t)^2}\left[\boldsymbol{u}_s(t+\Delta t) - \boldsymbol{u}_s(t)\right] - \frac{4}{\Delta t}\dot{\boldsymbol{u}}_s(t) - \ddot{\boldsymbol{u}}_s(t). \tag{19}$$

Substitution of these two expressions for $\dot{\boldsymbol{u}}_s(t+\Delta t)$ and $\ddot{\boldsymbol{u}}_s(t+\Delta t)$ into Eq. (17) gives:

$$\begin{aligned}\left[\frac{4}{(\Delta t)^2}\boldsymbol{M}_s + \frac{2}{\Delta t}\boldsymbol{C}_s + \boldsymbol{K}_s\right]\boldsymbol{u}_s(t+\Delta t)\\ = -\boldsymbol{M}_s\boldsymbol{R}_s\ddot{\boldsymbol{u}}_g(t+\Delta t) - \boldsymbol{c}\,\dot{\boldsymbol{u}}_b(t+\Delta t) - \boldsymbol{k}\,\boldsymbol{u}_b(t+\Delta t)\\ + \left[\frac{4}{(\Delta t)^2}\boldsymbol{M}_s + \frac{2}{\Delta t}\boldsymbol{C}_s\right]\boldsymbol{u}_s(t)\\ + \left[\frac{4}{\Delta t}\boldsymbol{M}_s + \boldsymbol{C}_s\right]\dot{\boldsymbol{u}}_s(t) + \boldsymbol{M}_s\ddot{\boldsymbol{u}}_s(t).\end{aligned} \tag{20}$$

In order to solve for $\boldsymbol{u}_s(t+\Delta t)$, first the base isolation system velocity vector at time $t + \Delta t$ has to be predicted. This vector can be computed in terms of displacement vectors using the three-point backward difference approximation [9]:

$$\dot{\boldsymbol{u}}_b(t+\Delta t) = \frac{1}{2\,\Delta t}\left[-4\,\boldsymbol{u}_b(t) + 3\boldsymbol{u}_b(t+\Delta t) + \boldsymbol{u}_b(t-\Delta t)\right]. \tag{21}$$

The error in the expression (21) is of order $(\Delta t)^2$.

The use of a modal representation for the superstructure, assumed to remain elastic, can reduce the computational cost of the nonlinear time history analysis.

3.3 Stability aspects

The proposed mixed explicit–implicit time integration method is conditionally stable because the second order central difference method is employed in the Explicit Integration Substep to compute the nonlinear response of the base isolation system. As will be shown in Sect. 4, in seismically isolated structures

the typical low stiffness value of the base isolation system generally allows one to have a critical time step Δt_{cr} larger than the short time step used to define the ground acceleration accurately.

Considering the 2D discrete structural model of a base-isolated structure with only linear isolation elements and neglecting the superstructure and base isolation system viscous damping, the dynamic equilibrium Eq. (11) at time t becomes:

$$m_b \ddot{u}_b(t) + \left(k_b + k_1\right) u_b(t) - k_1 u_1(t) = -m_b \ddot{u}_g(t) \,. \tag{22}$$

The superstructure first floor displacement u_1 can be expressed in terms of u_b as follows:

$$u_1 = u_b + \alpha\, u_b \,, \tag{23}$$

where the first term is the base isolation system displacement relative to the ground while the last term is the superstructure first floor displacement relative to the base isolation system; generally, the latter is very small compared to the former (i.e., $\alpha << 1$).

Dividing Eq. (22) by m_b, the dynamic equilibrium equation becomes:

$$\ddot{u}_b(t) + \frac{\left(k_b - \alpha\, k_1\right)}{m_b} u_b(t) = -\ddot{u}_g(t) \,. \tag{24}$$

Substituting the central difference expression for the acceleration at time t into Eq. (24) and solving for $u_b(t + \Delta t)$ gives:

$$u_b(t + \Delta t) = \left[2 - \frac{\Delta t^2}{m_b}\left(k_b - \alpha\, k_1\right)\right] u_b(t) - u_b(t - \Delta t) - \Delta t^2\, \ddot{u}_g(t) \,. \tag{25}$$

Equation (25) can be written as:

$$\left\{ \begin{array}{c} u_b(t + \Delta t) \\ u_b(t) \end{array} \right\} = \boldsymbol{A} \left\{ \begin{array}{c} u_b(t) \\ u_b(t - \Delta t) \end{array} \right\} - \boldsymbol{L}\, \ddot{u}_g(t) \,, \tag{26}$$

with:

$$\boldsymbol{A} = \left[\begin{array}{cc} 2 - \frac{\Delta t^2}{m_b}\left(k_b - \alpha\, k_1\right) & -1 \\ 1 & 0 \end{array} \right], \quad \boldsymbol{L} = \left\{ \begin{array}{c} \Delta t^2 \\ 0 \end{array} \right\},$$

where $\boldsymbol{A}$ and $\boldsymbol{L}$ are the integration approximation and load operators, respectively [2].

Since the stability of an integration method is determined by examining the behavior of the numerical solution for arbitrary initial conditions, it is possible to consider the integration of Eq. (22) when load is absent (i.e., $\ddot{u}_g = 0$).

In order to ca1culate the spectral radius of the approximation operator $\boldsymbol{A}$, the following eigenvalue problem has to be solved:

$$\left[\begin{array}{cc} 2 - \frac{\Delta t^2}{m_b}\left(k_b - \alpha\, k_1\right) & -1 \\ 1 & 0 \end{array} \right] \boldsymbol{u} \;=\; \lambda \boldsymbol{u} \,. \tag{27}$$

The eigenvalues are the roots of the characteristic polynomial $\rho(\lambda)$, defined as:

$$\rho(\lambda) = \left[2 - \frac{\Delta t^2}{m_b}\left(k_b - \alpha\, k_1\right) - \lambda\right](-\lambda) + 1 \,. \tag{28}$$

Hence:

$$\lambda_{1,2} = \frac{1}{2}\left[2 - \frac{\Delta t^2}{m_b}\left(k_b - \alpha\, k_1\right)\right] \pm \sqrt{\frac{1}{4}\left[2 - \frac{\Delta t^2}{m_b}\left(k_b - \alpha\, k_1\right)\right]^2 - 1} \,. \tag{29}$$

For stability the absolute values of λ_1 and λ_2 have to be smaller than or equal to 1 and this allows one to evaluate the critical time step Δt_{cr} of the Explicit Integration Substep:

$$\Delta t_{cr} = \frac{T}{\pi} = 2\sqrt{\frac{m_b}{k_b - \alpha\, k_1}} \,. \tag{30}$$

The same time step stability limit is also applicable when the viscous damping is not neglected [2].

It is important to note that the highest horizontal stiffness of each seismic isolator has to be used in order to evaluate Δt_{cr} and that α can be assumed equal to zero. In practice, since all isolation bearings are modeled by a bilinear model in which the post-yield stiffness is generally smaller than the initial elastic stiffness [23], the pre-yield stiffness of each isolator has to be chosen to determine Δt_{cr}.

Considering the 3D discrete structural model of a base-isolated structure, the critical time step Δt_{cr} can be evaluated considering the lower natural period given by the following eigenvalue problem:

$$\boldsymbol{k}_b^h \boldsymbol{\phi} = \boldsymbol{m}_b \boldsymbol{\phi}\, \boldsymbol{\Omega}^2 \,, \tag{31}$$

where $\boldsymbol{k}_b^h$ is the stiffness matrix of the base isolation system assembled using the highest horizontal stiffness of each nonlinear element.

4 Analysis of a 3D base-isolated structure

In the following, the nonlinear dynamic response of a 3D base-isolated structure subjected to bidirectional earthquake excitation is predicted using the proposed mixed explicit–implicit time integration method. The plane and the elevation of the analyzed structure are shown in Fig. 1.

The superstructure is a two-story reinforced concrete structure with vertical geometric irregularity, plan dimensions $2l_1 \, x \, 2l_2$, where $l_1 = 5$ m and $l_2 = 4$ m, and story height $h = 3.5$ m. The weight of the superstructure is 1802.9 kN and the first three natural periods are $T_{s1} = 0.15$ s, $T_{s2} = 0.14$ s and $T_{s3} = 0.10$ s, respectively. Each superstructure diaphragm mass includes the contributions of the dead load and live load on the floor diaphragm and the contributions of the structural elements and of the nonstructural elements between floors. As a result of the kinematic constraints assumed in Sect. 2.1 for the superstructure, the total number of the superstructure dofs, defined relative to the ground, is equal to 6.

The base isolation system, having a total weight of 914.9 kN, consists of seismic isolation bearings and a full diaphragm above the isolation devices. Because of the kinematic constraints adopted in Sect. 2.1 for the base isolation system, the total number of the isolation system dofs, defined relative to the ground, is equal to 3. Two types of base isolation systems are considered: base isolation system with lead rubber bearings (LRBS) and base isolation system with friction pendulum bearings (FPBS).

Bidirectional earthquake excitation is imposed with component SN and SP of the 1994 Northridge motion applied along directions X and Y of the global coordinate system, respectively. The ground acceleration record time step is 0.005 s. It is important to note that normally 200 points per second are used to define accurately an acceleration record, and that the time step of the ground motion can be reduced through linear interpolation because it is generally assumed that the acceleration function is linear within each time increment [34].

4.1 Dynamic response of the 3D base-isolated structure with lead rubber bearings

The base isolation system consists of 9 lead rubber bearings placed under the superstructure columns and modeled using a mathematical model capable of modeling both uniaxial and biaxial behavior of elastomeric and sliding bearings [24]. For the j-th elastomeric bearing, the nonlinear restoring forces along the orthogonal directions X and Y are described by the following equations:

$$\begin{aligned} f_{nx}^{(bj)} &= \alpha \frac{F_y}{y} u_x^{(bj)} + (1-\alpha) F_y z_x^{(bj)} \\ f_{ny}^{(bj)} &= \alpha \frac{F_y}{y} u_y^{(bj)} + (1-\alpha) F_y z_y^{(bj)} \end{aligned} \tag{32}$$

where α is the post-yield to the pre-yield stiffness ratio, F_y is the yield force and y is the yield displacement. The dimensionless variables $z_x^{(bj)}$ and $z_y^{(bj)}$ are governed by the following system of two differential equations proposed by Park et al. [27]:

$$\begin{Bmatrix} \dot{z}_x^{(bj)} y \\ \dot{z}_y^{(bj)} y \end{Bmatrix} = \begin{Bmatrix} A\dot{u}_x^{(bj)} \\ A\dot{u}_y^{(bj)} \end{Bmatrix} - \begin{bmatrix} \left(z_x^{(bj)}\right)^2 \left[\gamma \, sign\left(\dot{u}_x^{(bj)} z_x^{(bj)}\right) + \beta\right] & z_x^{(bj)} z_y^{(bj)} \left[\gamma \, sign\left(\dot{u}_y^{(bj)} z_y^{(bj)}\right) + \beta\right] \\ z_x^{(bj)} z_y^{(bj)} \left[\gamma \, sign\left(\dot{u}_x^{(bj)} z_x^{(bj)}\right) + \beta\right] & \left(z_y^{(bj)}\right)^2 \left[\gamma \, sign\left(\dot{u}_y^{(bj)} z_y^{(bj)}\right) + \beta\right] \end{bmatrix} \begin{Bmatrix} \dot{u}_x^{(bj)} \\ \dot{u}_y^{(bj)} \end{Bmatrix}, \tag{33}$$

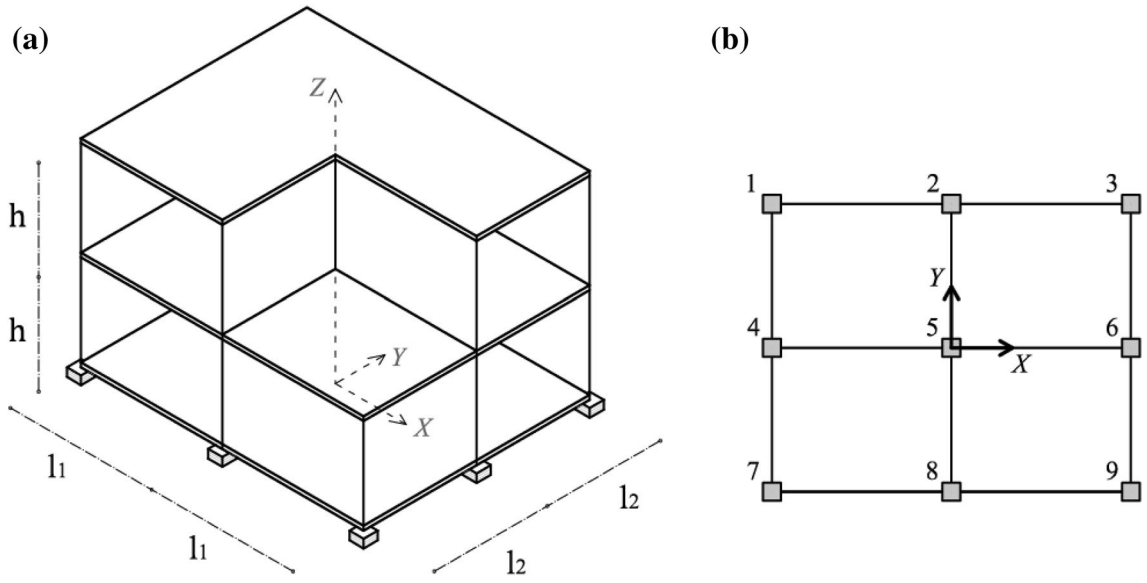

Fig. 1 Two-story reinforced concrete base-isolated structure: **a** elevation; **b** plan

in which A, γ and β are dimensionless quantities that control the shape of the hysteresis loop. Furthermore, $u_x^{(bj)}$, $u_y^{(bj)}$ and $\dot{u}_x^{(bj)}$, $\dot{u}_y^{(bj)}$ are the displacements and velocities that occur at the j-th isolation device, respectively. Constantinou et al. [8] have shown that the interaction curve between the nonlinear restoring forces in the two directions is circular only when the condition $A/(\gamma+\beta)=1$ is satisfied; accordingly, in the present study, $A=1$, $\gamma=0.5$ and $\beta=0.5$. The unconditionally stable semi-implicit Runge–Kutta method [31] is employed to solve the differential equations governing the behavior of each nonlinear isolation element with a number of steps equal to 50.

The base isolation system has been designed in order to provide an effective isolation period $T_{eff}=2.25$ s and an effective viscous damping $\upsilon_{eff}=0.15$ at the design displacement $D_d=0.50$ m. Each elastomeric bearing has a yield force $F_y=31422$ N, a yield displacement $y=0.017$ m and a post-yield to pre-yield stiffness ratio $\alpha=0.10$.

Tables 1 and 2 compare the maximum and minimum displacements of the base isolation system mass center MC_b and the maximum and minimum accelerations, relative to the ground, of the second story mass center MC_2 in X and Y directions, obtained for two different values of time step using the proposed Mixed Explicit–Implicit time integration Method (MEIM) and the Pseudo-Force Method (PFM), both implemented on the same computer (Intel® Core™ i7-4700MQ processor, CPU at 2.40 GHz with 16 GB of RAM) by using the computer program Matlab and verified using SAP2000. In the pseudo-force method the adopted convergence tolerance value is equal to 10^{-8}.

The two values of time step used in the Nonlinear Time History Analyses (NLTHAs) are 0.005 and 0.001 s. Since the critical time step Δt_{cr}, evaluated using Eq. (30) and considering the lower natural period given by the eigenvalue problem in Eq. (31), is equal to 0.32 s, it is clear that there are no stability problems. Note that the mixed explicit–implicit time integration method continues to reduce the computational effort even when a smaller time step, which allows one to minimize the error in Eqs. (16) and (21), is used (i.e. $\Delta t=0.001$ s). It must be emphasized that the comparisons using the total computational time *tct* are meaningful only qualitatively because it depends on the CPU speed, memory capability and background processes of the computer used to obtain the previous results. To this end, in order to normalize the computational time results, Tables 1 and 2 also show the percentage of the MEIM total computational time evaluated with respect to the PFM *tct* as follows: *tctp* [%] = (MEIM *tct* / PFM *tct*) · 100 .

The two plots in Fig. 2 show the nonlinear restoring force–displacement hysteresis loop of Isolator 1, illustrated in Fig. 1b, in the X and Y directions, respectively.

4.2 Dynamic response of the 3D base-isolated structure with friction pendulum bearings

The base isolation system consists of 9 friction pendulum bearings placed under the superstructure columns and modeled using the previous mathematical model [24]. For a friction pendulum bearing, the nonlinear restoring forces along the orthogonal directions X and Y are described by the following equations:

$$f_{nx}^{(bj)}=\frac{N^{(bj)}}{R}u_x^{(bj)}+\mu N^{(bj)}z_x^{(bj)}\quad f_{ny}^{(bj)}=\frac{N^{(bj)}}{R}u_y^{(bj)}+\mu N^{(bj)}z_y^{(bj)}, \tag{34}$$

in which $N^{(bj)}$ is the vertical load carried by the j-th bearing, μ is the coefficient of sliding friction which depends on the bearing pressure and the instantaneous velocity of sliding, $z_x^{(bj)}$ and $z_y^{(bj)}$ are dimensionless variables governed by the system of two differential equations given in Eq. (33).

The base isolation system has been designed in order to provide an effective isolation period $T_{eff}=2.25$ s and an effective viscous damping $\upsilon_{eff}=0.10$ at the design displacement $D_d=0.50$ m. Each bearing has a radius of

Table 1 NLTHAs results with $\Delta t=0.005$ s (LRBS)

	tct (s)	*tctp* (%)	$u_x^{(MC_b)}$ (m)		$u_y^{(MC_b)}$ (m)		$\ddot{u}_x^{(MC_2)}$ (g)		$\ddot{u}_y^{(MC_2)}$ (g)	
			max	min	max	min	max	min	max	min
MEIM	45	18.44	0.3332	− 0.3327	0.2286	− 0.1787	0.5293	− 0.4586	1.0986	− 1.0783
PFM	244	–	0.3330	− 0.3327	0.2287	− 0.1787	0.5456	− 0.4624	1.0874	− 1.0399

Table 2 NLTHAs results with $\Delta t=0.001$ s (LRBS)

	tct (s)	*tctp* (%)	$u_x^{(MC_b)}$ (m)		$u_y^{(MC_b)}$ (m)		$\ddot{u}_x^{(MC_2)}$ (g)		$\ddot{u}_y^{(MC_2)}$ (g)	
			max	min	max	min	max	min	max	min
MEIM	220	26.79	0.3341	− 0.3333	0.2292	− 0.1794	0.5415	− 0.4705	1.1285	− 1.0728
PFM	821	–	0.3341	− 0.3333	0.2292	− 0.1794	0.5418	− 0.4701	1.1274	− 1.0743

curvature of the spherical concave surface $R = 1.25$ m, a sliding friction coefficient $\mu = 0.07$ and a yield displacement $y = 0.0002$ m. In this work, the vertical load $N^{(bj)}$ is assumed equal to the weight $W^{(bj)}$ acting on the j-th isolator and the dependency of the sliding friction coefficient on bearing pressure and sliding velocity is neglected.

Tables 3 and 4 compare the maximum and minimum displacements of the base isolation system mass center MC_b and the maximum and minimum accelerations, relative to the ground, of the second story mass center MC_2 in X and Y directions, obtained for two different values of the time step using the proposed mixed explicit–implicit time integration method (MEIM) and the pseudo-force method (PFM).

The two values of time step used in the nonlinear time history analyses are 0.005 and 0.001 s. Since the critical time step Δt_{cr}, evaluated using Eq. (30) and considering the lower natural period given by the eigenvalue problem in Eq. (31), is equal to 0.015 s, it is evident that in this case, even if friction pendulum bearings have a very high initial stiffness value, there are no stability problems. It is important to note that the mixed explicit–implicit time integration method continues to reduce significantly the total computational effort even when a smaller time step is used (i.e. $\Delta t = 0.001$ s). Specifically, according to Tables 3 and 4, the mixed explicit–implicit method, performed with the smallest time step ($\Delta t = 0.001$ s), requires less computational effort than the pseudo-force method even if the latter is performed using the largest time step ($\Delta t = 0.005$ s): indeed, the MEIM total computational time percentage, referred to the PFM *tct* evaluated adopting $\Delta t = 0.005$ s, is equal to 38.46%. It transpires that even when the time step size arising from stability requirements becomes smaller than the one used to define the ground acceleration accurately, as in the case of base isolation systems having isolators with very high initial stiffness (i.e., sliding bearings) or very high stiffness at large displacements (i.e., high damping rubber bearings), the proposed method preserves its computational efficiency with respect to conventional implicit time integration methods.

The two plots in Fig. 3 show the nonlinear restoring force–displacement hysteresis loop of the Isolator 1, illustrated in Fig. 1b, in the X and Y directions, respectively.

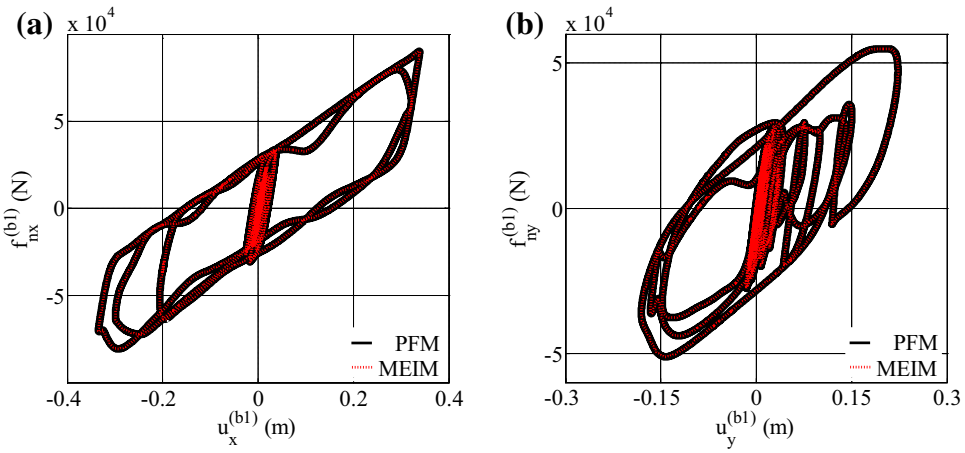

Fig. 2 Nonlinear restoring force–displacement hysteresis loop of isolator 1: **a** X; **b** Y directions

Table 3 NLTHAs results with $\Delta t = 0.005$ s (FPBS)

	tct (s)	*tctp* (%)	$u_x^{(MC_b)}$ (m)		$u_y^{(MC_b)}$ (m)		$\ddot{u}_x^{(MC_2)}$ (g)		$\ddot{u}_y^{(MC_2)}$ (g)	
			max	min	max	min	max	min	max	min
MEIM	47	7.86	0.3312	− 0.3138	0.2831	− 0.2507	0.4708	− 0.4772	1.1883	− 0.9682
PFM	598	–	0.3310	− 0.3137	0.2829	− 0.2505	0.4729	− 0.4164	1.0778	− 1.1374

Table 4 NLTHAs results with $\Delta t = 0.001$ s (FPBS)

	tct (s)	*tctp* (%)	$u_x^{(MC_b)}$ (m)		$u_y^{(MC_b)}$ (m)		$\ddot{u}_x^{(MC_2)}$ (g)		$\ddot{u}_y^{(MC_2)}$ (g)	
			max	min	max	min	max	min	max	min
MEIM	230	18.54	0.3312	− 0.3139	0.2832	− 0.2507	0.4779	− 0.4692	1.2015	− 0.9925
PFM	1240	–	0.3312	− 0.3139	0.2832	− 0.2507	0.4783	− 0.4693	1.2067	− 0.9835

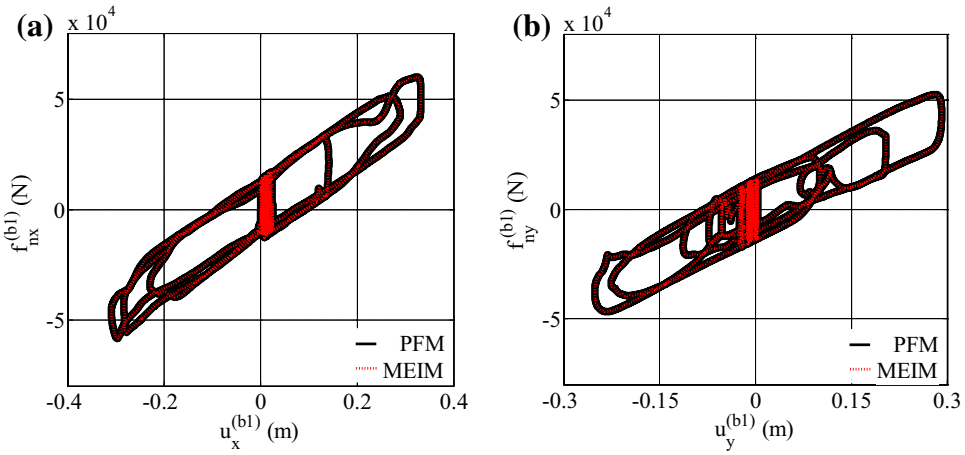

Fig. 3 Nonlinear restoring force–displacement hysteresis loop of isolator 1: **a** X; **b** Y directions

5 Conclusions

In this paper, the accuracy, the stability and the computational efficiency of a mixed explicit–implicit time integration method (MEIM) proposed for predicting the nonlinear response of base-isolated structures subjected to earthquake excitation have been investigated. Adopting the partitioned solution approach, currently used in most practical civil engineering problems due to the increasing complexity of structural models, the discrete structural model of a typical 3D base-isolated structure has been decomposed into two substructures, namely superstructure and base isolation system. Being the base isolation system much more flexible than the superstructure to decouple the latter from the earthquake ground motion, an explicit conditionally stable time integration method (i.e., central difference method) has been employed to evaluate the nonlinear base isolation system response and an implicit unconditionally stable time integration method (i.e., Newmark's constant average acceleration method) has been adopted to predict the linear superstructure response with the remarkable benefit in avoiding the iterative procedure within each time step of a nonlinear time history analysis required by conventional implicit time integration methods.

The dynamic response of a 3D base-isolated structure subjected to bidirectional earthquake excitation has been analyzed using the proposed mixed explicit–implicit method. Two types of base isolation systems have been considered, namely, base isolation system with lead rubber bearings (LRBS) and base isolation system with friction pendulum bearings (FPBS), in order to investigate the use of the mixed time integration procedure also in the presence of isolators with very high initial stiffness such as the latter ones. The accuracy and the computational efficiency of the proposed mixed explicit–implicit method have been assessed by comparing the results with those obtained by using the two-step solution algorithm developed specifically for the analysis of base-isolated structures by Nagarajaiah et al. [24]. For brevity, in this paper, this implicit time integration method adopted in conjunction with the pseudo-force approach has been referred to as the Pseudo-Force Method (PFM).

From the numerical results presented in the paper, the following conclusions can be drawn:

- As regards the accuracy, the proposed mixed explicit–implicit time integration method provides results that are close enough to those obtained adopting the pseudo-force method, for both two values of time step adopted in the nonlinear time history analyses of the 3D base-isolated structure with LRBS and FPBS. Both numerical methods, implemented on the same computer by using the computer program Matlab, have been verified using SAP2000.
- As far as the stability is concerned, the proposed mixed explicit–implicit time integration method is conditionally stable because the central difference method is employed to predict the nonlinear response of the base isolation system. The low stiffness value of the base isolation system with lead rubber bearings (LRBS) allows one to have a critical time step considerably larger than the imposed ground acceleration record time step. Furthermore, the critical time step continues to be larger than the ground acceleration time step also in the case of base isolation system with friction pendulum bearings (FPBS) in spite of their very high initial stiffness.
- Regarding the computational efficiency, the total computational time, *tct*, required by the mixed explicit–implicit time integration method is significantly reduced in comparison to the pseudo-force method: the MEIM *tct* evaluated with respect to the PFM *tct* for a $\Delta t = 0.005$ s is equal to 18.44 % in the LRBS case and equal to 7.86 % in the FPBS case. In addition, the mixed explicit–implicit time integration method, performed with the smallest time step ($\Delta t = 0.001$ s), requires less computational effort than the

pseudo-force method even if the latter is performed using the largest time step ($\Delta t = 0.005$ s): indeed, the MEIM total computational time percentage, referred to the PFM *tct* evaluated adopting $\Delta t = 0.005$ s, is equal to 90.20% in the LRBS case and equal to 38.46% in the FPBS case. It transpires that even when the critical time step size arising from stability requirements becomes smaller than the one used to define the ground acceleration accurately, as in the case of base isolation systems having isolators with very high initial stiffness (i.e., sliding bearings) or very high stiffness at large displacements (i.e., high damping rubber bearings), the proposed method preserves its computational efficiency with respect to conventional implicit time integration methods.

It follows that the proposed mixed explicit–implicit time integration method can be effectively adopted in the context of earthquake engineering structural applications being a very efficient solution approach for the nonlinear time history analysis of base-isolated structures under seismic loads.

Appendix: solution algorithm

The proposed solution algorithm is given in the following:

1. Initial calculations:
   - 1.1 Form superstructure mass matrix $\boldsymbol{M}_s$, damping matrix $\boldsymbol{C}_s$ and stiffness matrix $\boldsymbol{K}_s$ and base isolation system mass matrix $\boldsymbol{m}_b$, damping matrix $\boldsymbol{c}_b$ and stiffness matrix $\boldsymbol{k}_b$.
   - 1.2 Initialize superstructure displacement, velocity and acceleration vectors $\boldsymbol{u}_s(0)$, $\dot{\boldsymbol{u}}_s(0)$, $\ddot{\boldsymbol{u}}_s(0)$, and base isolation system displacement, velocity and acceleration vectors $\boldsymbol{u}_b(0)$, $\dot{\boldsymbol{u}}_b(0)$, $\ddot{\boldsymbol{u}}_b(0)$; then calculate:

$$\boldsymbol{u}_b(-\Delta t) = \boldsymbol{u}_b(0) - \Delta t\, \dot{\boldsymbol{u}}_b(0) + \frac{(\Delta t)^2}{2}\ddot{\boldsymbol{u}}_b(0)\,.$$

   - 1.3 Select time step Δt, $\Delta t \leqslant \Delta t_{cr}$, and calculate the integration constants:

$$a_1 = \frac{2}{(\Delta t)^2} \quad a_2 = \frac{1}{(\Delta t)^2} \quad a_3 = \frac{1}{2\Delta t} \quad a_4 = \frac{4}{(\Delta t)^2}$$
$$a_5 = \frac{2}{\Delta t} \quad a_6 = \frac{4}{\Delta t}\,.$$

   - 1.4 Form effective mass matrix and effective stiffness matrix:

$$\boldsymbol{M}^* = a_2\,\boldsymbol{m}_b + a_3\,\left(\boldsymbol{c}_b + \boldsymbol{c}_1\right)$$
$$\boldsymbol{K}^* = a_4\,\boldsymbol{M}_s + a_5\,\boldsymbol{C}_s + \boldsymbol{K}_s\,.$$

   - 1.5 Triangularize $\boldsymbol{M}^*$ and $\boldsymbol{K}^*$:

$$\boldsymbol{M}^* = \boldsymbol{L}_{\mathrm{e}}\,\boldsymbol{D}_{\mathrm{e}}\,\boldsymbol{L}_e^{\mathrm{T}}$$
$$\boldsymbol{K}^* = \boldsymbol{L}_{\mathrm{i}}\,\boldsymbol{D}_{\mathrm{i}}\,\boldsymbol{L}_i^{\mathrm{T}}\,.$$

2. Calculations for each time step:
   - 2.1 Compute the state of motion at each seismic isolation bearing at time t.
   - 2.2 Compute the resultant nonlinear forces vector $\boldsymbol{f}_n(t)$ at the center of mass of the base isolation system.
   - 2.3 Calculate the explicit integration substep effective load vector at time t:

$$\begin{aligned}\boldsymbol{P}_e^*(t) = &-\boldsymbol{m}_b\boldsymbol{R}_b\ddot{\boldsymbol{u}}_g(t) - \boldsymbol{c}^T\dot{\boldsymbol{u}}_s(t) - \boldsymbol{k}^T\boldsymbol{u}_s(t) - \boldsymbol{f}_n(t)\\ &+ \left[a_1\boldsymbol{m}_b - \boldsymbol{k}_b - \boldsymbol{k}_1\right]\boldsymbol{u}_b(t)\\ &+ \left[-a_2\boldsymbol{m}_b + a_3\left(\boldsymbol{c}_b + \boldsymbol{c}_1\right)\right]\boldsymbol{u}_b(t-\Delta t)\,.\end{aligned}$$

   - 2.4 Solve for base isolation system displacement vector at time $t + \Delta t$:

$$\boldsymbol{L}_e\boldsymbol{D}_e\boldsymbol{L}_e^T\,\boldsymbol{u}_b(t+\Delta t) = \boldsymbol{P}_e^*(t)\,.$$

   - 2.5 Evaluate base isolation system velocity and acceleration vectors at time t:

$$\dot{\boldsymbol{u}}_b(t) = a_3\,\left[\boldsymbol{u}_b(t+\Delta t) - \boldsymbol{u}_b(t-\Delta t)\right]$$
$$\ddot{\boldsymbol{u}}_b(t) = a_2\,\left[\boldsymbol{u}_b(t+\Delta t) - 2\boldsymbol{u}_b(t) + \boldsymbol{u}_b(t-\Delta t)\right]\,.$$

   - 2.6 Calculate the implicit integration substep effective load vector at time $t + \Delta t$:

$$\begin{aligned}\boldsymbol{P}_i^*(t+\Delta t) = &-\boldsymbol{M}_s\boldsymbol{R}_s\ddot{\boldsymbol{u}}_g(t+\Delta t) - a_3\,\boldsymbol{c}\,\left[-4\,\boldsymbol{u}_b(t)\right.\\ &\left.+3\boldsymbol{u}_b(t+\Delta t) + \boldsymbol{u}_b(t-\Delta t)\right] - \boldsymbol{k}\,\boldsymbol{u}_b(t+\Delta t)\\ &+ \left[a_4\boldsymbol{M}_s + a_5\boldsymbol{C}_s\right]\boldsymbol{u}_s(t) + \left[a_6\boldsymbol{M}_s + \boldsymbol{C}_s\right]\dot{\boldsymbol{u}}_s(t)\\ &+ \boldsymbol{M}_s\ddot{\boldsymbol{u}}_s(t)\,.\end{aligned}$$

   - 2.7 Solve for superstructure displacement vector at time $t + \Delta t$:

$$\boldsymbol{L}_i\boldsymbol{D}_i\boldsymbol{L}_i^T\,\boldsymbol{u}_s(t+\Delta t) = \boldsymbol{P}_i^*(t+\Delta t)\,.$$

   - 2.8 Evaluate superstructure velocity and acceleration vectors at time $t + \Delta t$:

$$\dot{\boldsymbol{u}}_s(t+\Delta t) = a_5\left[\boldsymbol{u}_s(t+\Delta t) - \boldsymbol{u}_s(t)\right] - \dot{\boldsymbol{u}}_s(t)$$
$$\ddot{\boldsymbol{u}}_s(t+\Delta t) = a_4\left[\boldsymbol{u}_s(t+\Delta t) - \boldsymbol{u}_s(t)\right] - a_6\,\dot{\boldsymbol{u}}_s(t) - \ddot{\boldsymbol{u}}_s(t)\,.$$

3. Repetition for next time step: replace t by $t + \Delta t$ and repeat steps 2.1–2.8 for the next time step.

References

1. Alhan C, Gavin H (2004) A parametric study of linear and nonlinear passively damped seismic isolation systems for buildings. Eng Struct 26:485–497
2. Bathe KJ (1996) Finite element procedures. Prentice-Hall, Upper Saddle River
3. Belytschko T, Yen HJ, Mullen R (1979) Mixed methods for time integration. Comput Methods Appl Mech Eng 17/18:259–275
4. Bozorgnia Y, Bertero VV (2004) Earthquake engineering: from engineering seismology to performance-based engineering. CRC Press, New York
5. Brun M, Batti A, Limam A, Gravouil A (2012) Explicit/implicit multi-time step co-computations for blast analyses on a reinforced concrete frame structure. Finite Elem Anal Des 52:41–59
6. Chopra AK (2012) Dynamics of structures: theory and applications to earthquake engineering, 4th edn. Prentice Hall, Englewood Cliffs
7. Combescure A, Gravouil A (2002) A numerical scheme to couple subdomains with different time-steps for predominantly linear transient analysis. Comput Methods Appl Mech Eng 191:1129–1157
8. Constantinou MC, Mokha A, Reinhorn AM (1990) Teflon bearings in base isolation II: modeling. J Struct Eng ASCE 116(2):455–474
9. D'Acunto B (2012) Computational partial differential equations for engineering science. Nova Science Publishers, New York
10. Dokainish MA, Subbaraj K (1989) A survey of direct time-integration methods in computational structural dynamics—I. Explicit methods. Comput Struct 32(6):1371–1386
11. Dokainish MA, Subbaraj K (1989) A Survey of direct time-integration methods in computational structural dynamics—II. Implicit methods. Comput Struct 32(6):1387–1401
12. Farhat C, Crivelli L, Roux FX (1994) A transient FETI methodology for large-scale parallel implicit computations in structural mechanics. Int J Numer Methods Eng 37:1945–1975
13. Farhat C, Roux FX (1991) A method of finite element tearing and interconnecting and its parallel solution algorithm. Int J Numer Methods Eng 32:1205–1227
14. Felippa CA, Park KC, Farhat C (2001) Partitioned analysis of coupled mechanical systems. Comput Methods Appl Mech Eng 190:3247–3270
15. Gravouil A, Combescure A (2001) Multi-time-step explicit-implicit method for non-linear structural dynamics. Int J Numer Methods Eng 50:199–225
16. Herry B, Di Valentin L, Combescure A (2002) An approach to the connection between subdomains with non-matching meshes for transient mechanical analysis. Int J Numer Methods Eng 55:973–1003
17. Hughes TJR, Liu WK (1978) Implicit–explicit finite elements in transient analysis: implementation and numerical examples. J Appl Mech 45:375–378
18. Jangid RS, Datta TK (1995) Performance of base isolation systems for asymmetric building subject to random excitation. Eng Struct 17(6):443–454
19. Kelly JM (1997) Earthquake-resistant design with rubber, 2nd edn. Springer, Berlin
20. Krieg RD (1973) Unconditional stability in numerical time integration methods. J Appl Mech 40:417–421
21. Muscolino G (1990) Dynamic response of multiply connected primary–secondary systems. Earthq Eng Struct Dyn 19:205–216
22. Naeim F (2001) The seismic design handbook, 2nd edn. Springer, New York
23. Naeim F, Kelly JM (1999) Design of seismic isolated structures: from theory to practice. Wiley, Hoboken
24. Nagarajaiah S, Reinhorn AM, Constantinou MC (1991) Nonlinear dynamic analysis of 3-D base-isolated structures. J Struct Eng ASCE 117(7):2035–2054
25. Noh G, Bathe KJ (2013) An explicit time integration scheme for the analysis of wave propagations. Comput Struct 129:178–193
26. Noh G, Ham S, Bathe KJ (2013) Performance of an implicit time integration scheme in the analysis of wave propagations. Comput Struct 123:93–105
27. Park YJ, Wen YK, Ang AHS (1986) Random vibration of hysteretic systems under bi-directional ground motions. Earthq Eng Struct Dyn 14:543–557
28. Pezeshk S, Camp CV (1995) An explicit time integration technique for dynamics analyses. Int J Numer Methods Eng 38:2265–2281
29. Quarteroni A (2014) Numerical models for differential problems, 2nd edn. Springer, Milano
30. Quarteroni A, Valli A (1999) Domain decomposition methods for partial differential equations. Oxford Science Publications, Oxford
31. Rosenbrock HH (1963) Some general implicit processes for the numerical solution of differential equations. Comput J 5:329–330
32. Vaiana N, Filippou FC, Serino G (2017) Nonlinear dynamic analysis of base-isolated structures using a partitioned solution approach and an exponential model. Int J Civ Environ Eng 11(2), 2017, Conference paper of the 19th International Conference on Earthquake and Structural Engineering (ICESE 2017), London, UK, February 16–17, 2017
33. Vaiana N, Filippou FC, Serino G (2017) Nonlinear dynamic analysis of base-isolated structures using a mixed integration method: stability aspects and computational efficiency. Int J Civ Environ Eng 11(2), 2017, Conference paper of the 19th International Conference on Earthquake Engineering, Barcelona, Spain, February 26–27, 2017
34. Wilson EL (2002) Three-dimensional static and dynamic analysis of structures, 3rd edn. Computers and Structures Inc, Berkeley
35. Wu YS, Smolinski P (2000) A multi-time step integration algorithm for structural dynamics based on the modified trapezoidal rule. Comput Methods Appl Mech Eng 187:641–660